

Supporting Information:

**SERS-Enhanced Piezoplasmonic Graphene Composite for Biological and Structural Strain Mapping**

Brandon C. Marin, Justin Liu, Eden Aklile, Armando Urbina, Andrew S-C. Chiang,

Natalie Lawrence, Shaochen Chen, Darren J. Lipomi\*

Department of NanoEngineering, University of California, San Diego

9500 Gilman Drive, Mail Code 0448, La Jolla, CA 92093-0448

\*Author to whom correspondence should be addressed: [dlipomi@ucsd.edu](mailto:dlipomi@ucsd.edu)

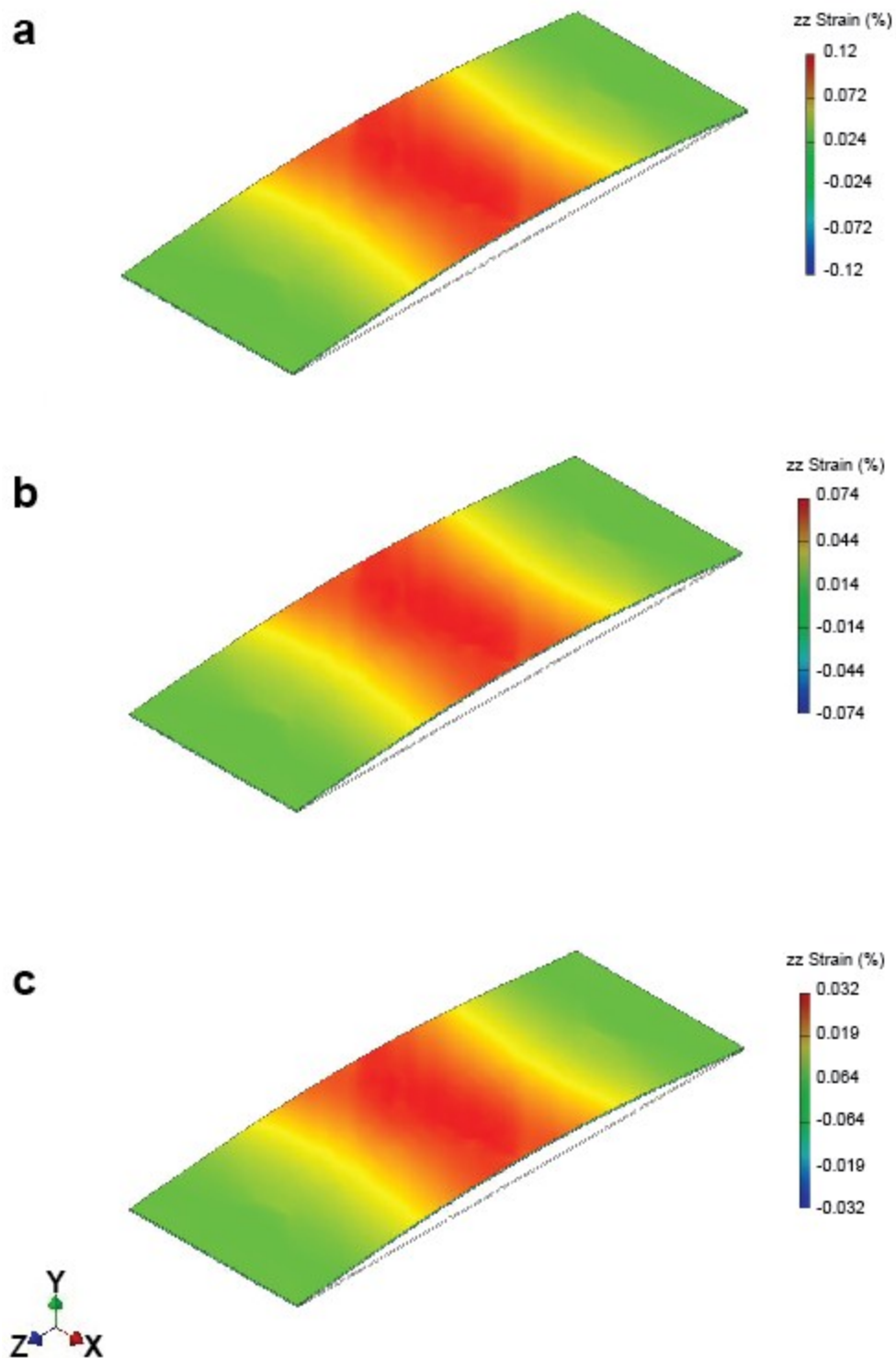


**Figure S1: Finite-Element Simulation of Strained Glass slide.** The strain distribution (zz-component) of bent 50.8 mm x 19.05 mm x 0.20 mm glass slides is depicted. The strain at the apex (in y-direction) of the glass slides is 0.12 % (a), 0.074 % (b), and 0.032 % (c). Note that direction orthogonal to the glass slide is defined as the y-direction.

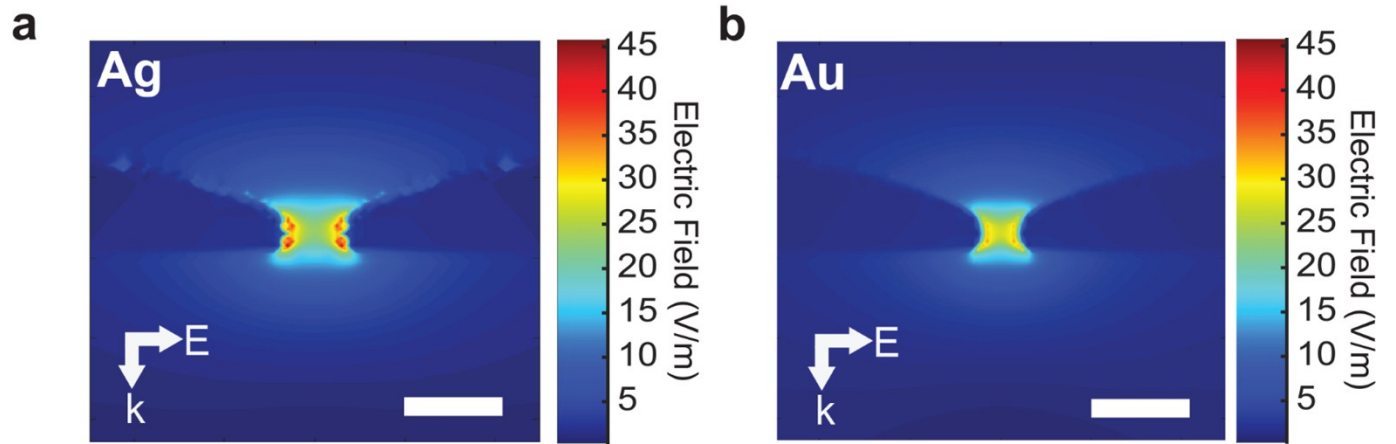


**Figure S2: Two-dimensional finite-difference time-domain (FDTD) simulations of gaps between noble metal nanoislands.** The electric field magnitude is plotted in 2D space for silver (a) and gold (b) nanoislands with a 5 nm gap under 633 nm excitation. Nanoislands are on a 3-Å thick monolayer of graphene supported by silica. Scale bars are 10 nm. The polarization and propagation of incident light is defined by the white arrows. The simulated nanoisland shape was approximated by SEM and TEM images.

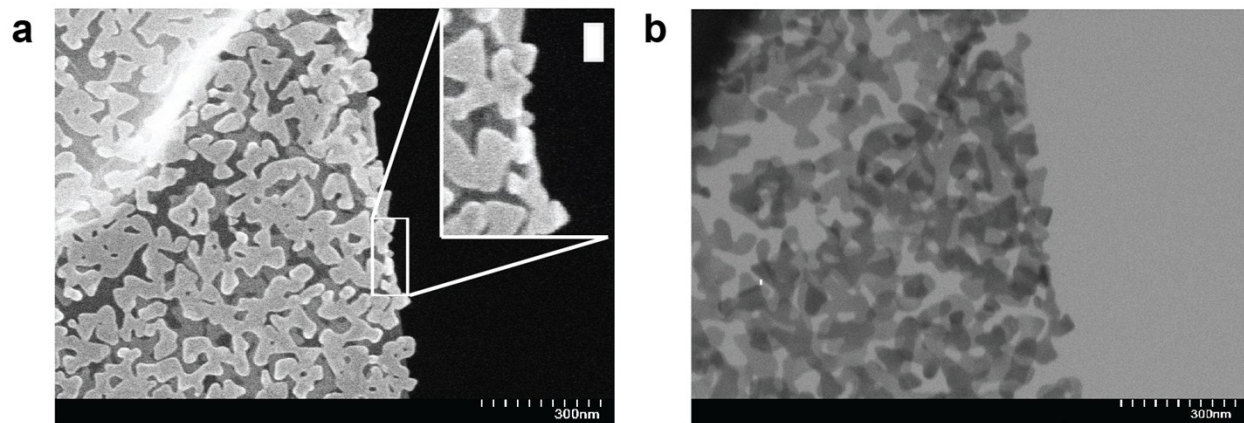


**Figure S3: Scanning/Transmission Electron Micrographs of Gold Nanoislands.** Electron micrographs of folded over gold nanoisland on graphene film are depicted in scanning (a) and transmission (b) modes. The samples are free standing on a TEM copper grid and only supported by the graphene monolayer. The inset in a) depicts the side profile of metal nanoislands (scale bar 20 nm).

z-distance from apex (mm)	Slide A zz-Strain (%)	Slide B zz-Strain (%)	Slide C zz-Strain (%)
0.00	0.11790	0.07272	0.03150
0.25	0.11740	0.07239	0.03131
0.50	0.11640	0.07176	0.03103
0.75	0.11540	0.07114	0.03076
1.00	0.11460	0.07068	0.03057
1.25	0.11410	0.07034	0.03042
1.50	0.11330	0.06985	0.03021
1.75	0.11230	0.06926	0.02995
2.00	0.11140	0.06873	0.02972
2.25	0.11060	0.06823	0.02951
2.50	0.11020	0.06796	0.02390
2.75	0.10980	0.06770	0.02928
3.00	0.10920	0.06734	0.02912
3.25	0.18500	0.06694	0.02895
3.50	0.10790	0.06654	0.02878
3.75	0.10680	0.06589	0.02885
4.00	0.10580	0.06529	0.02240
4.25	0.10480	0.06468	0.02797
4.50	0.10360	0.06391	0.02764
4.75	0.10230	0.06308	0.02728
5.00	0.10090	0.06226	0.02692

**Table S1: Strain Values along Length of Glass Slides.** Strain values as a function of distance from the apex are depicted as obtained from finite-element simulations. Slides A, B, and C correspond to slides with a maximal strain of 0.12, 0.072, and 0.032 %, respectively.

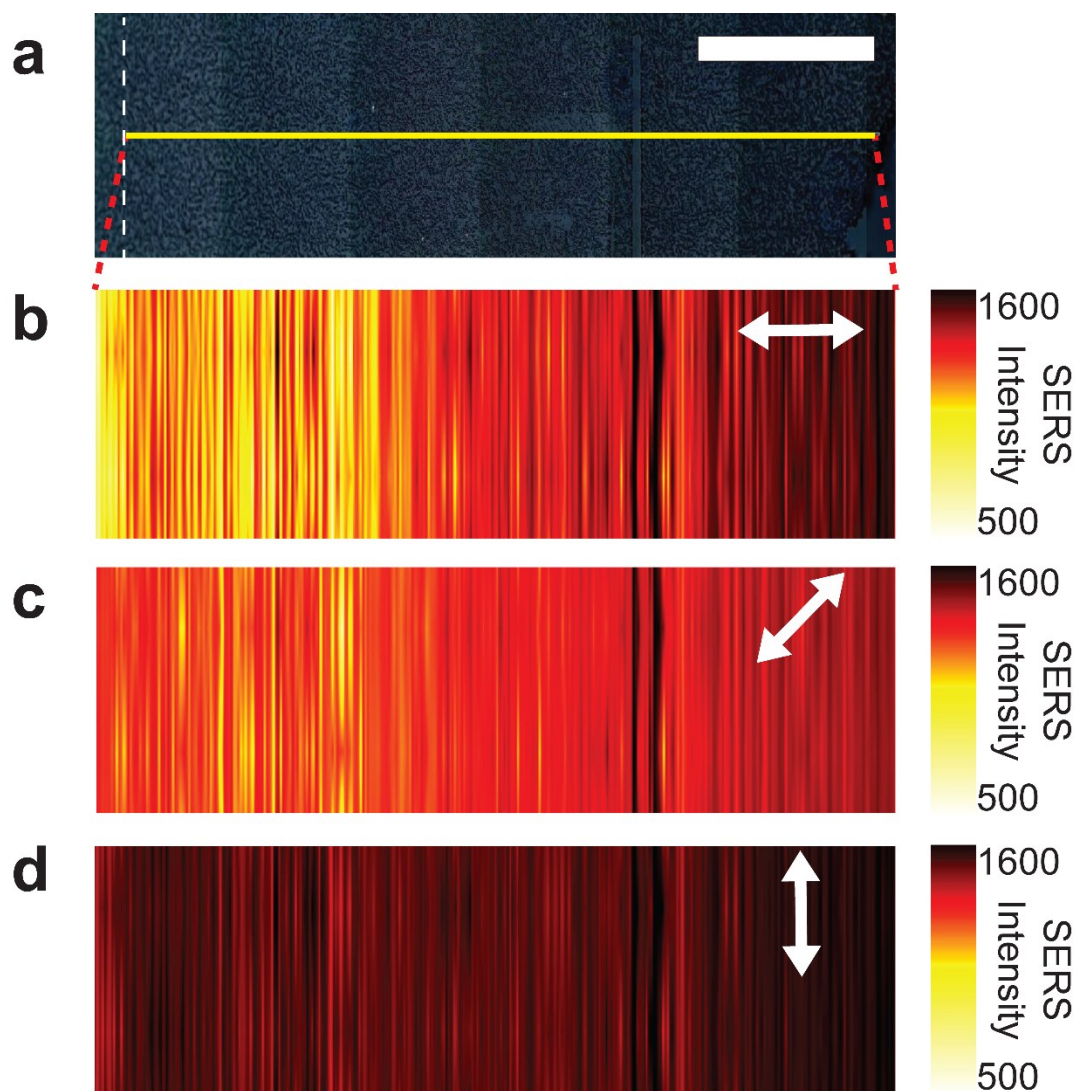


**Figure S4: 2D Raman mapping of strain gradients using a bent glass substrate bearing silver nanoislands on graphene.** A bright-field image (a) of AgNIs on a bent glass substrate is shown. Scale bar is 500  $\mu\text{m}$ . The yellow box near the center of the image is the selected area ( $2100 \mu\text{m} \times 6 \mu\text{m}$ ) that was mapped using a Raman microscope. The apex of the bent substrate is marked by the dotted white lines and has a strain of 0.032%. (b-d) Raman maps of the selected area under various polarizations ( $0^\circ$ ,  $45^\circ$ , and  $90^\circ$  respectively) of the electric field. Polarization is denoted by the white arrows and the legend shows the intensity of the Raman signal. Vertical artifacts in Raman maps are due to overlapping samples in horizontal rastering of collected signal.

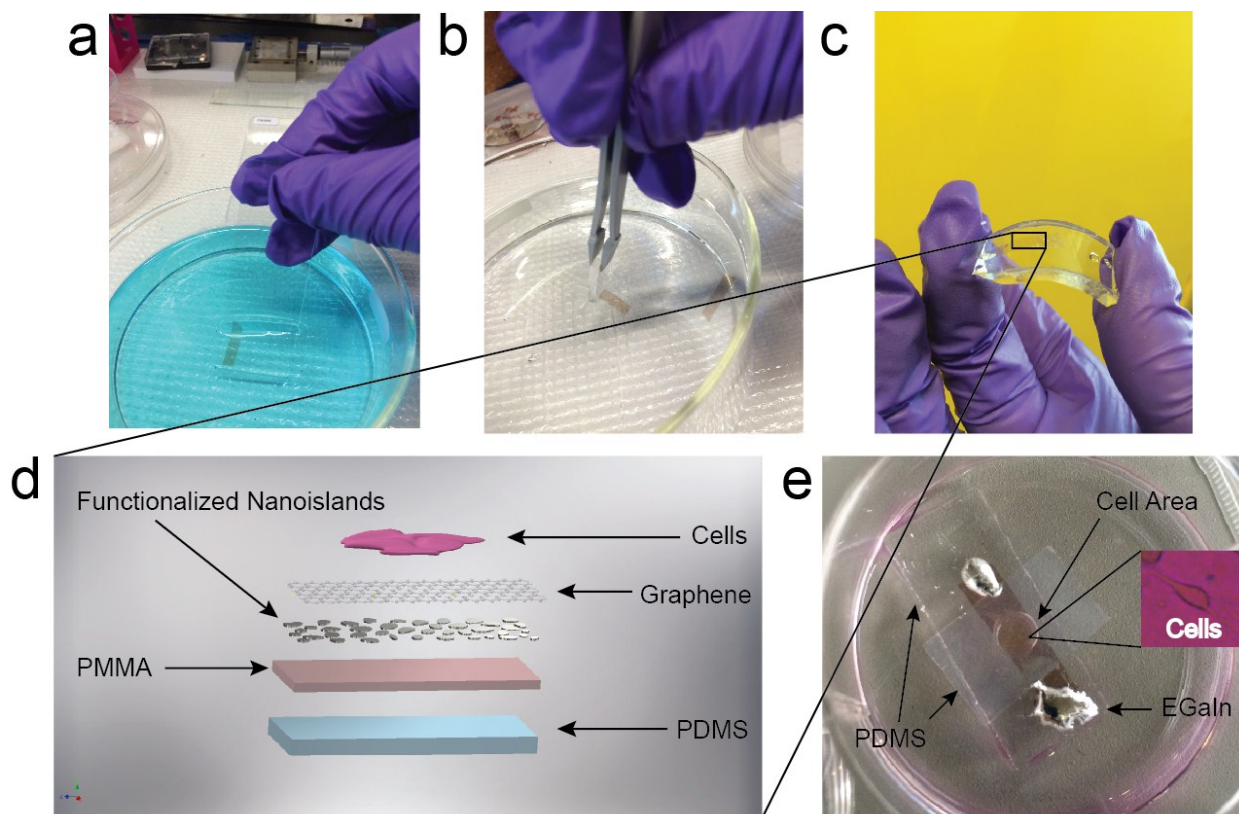


**Figure S5: Silver Nanoislands for Musculoskeletal Cell Strain Detection.** Camera images showing transfer of PMMA/ $\text{NI}_{\text{func}}$ /Gr samples onto glass from ammonia persulfate etching solution (a). Samples are transferred into a clean DI water container and transferred onto a PDMS slab graphene side up (b). Once on PDMS samples are remarkably flexible (c). A diagram showing the layers of the sample on the PDMS is depicted (d). A camera image of the final substrate with cells is shown in (e), note that there is a PDMS barrier added to contain liquid media to feed the cells and EGaIn contacts on the ends for electrical addressing. The inset in (e) depicts a myoblast cell image for illustrative purposes.



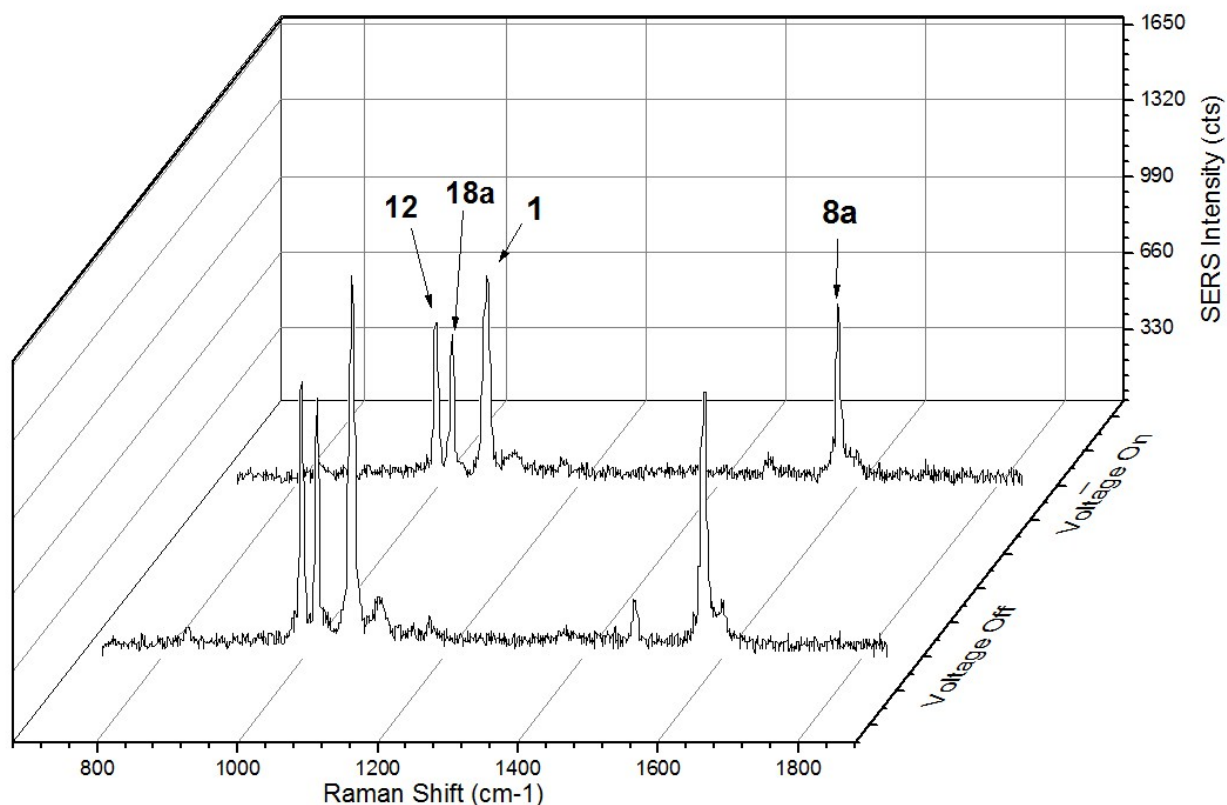


**Figure S6: SERS spectra of myoblast cells on an inverted silver nanoisland substrate.** The SERS spectra of benzenethiolate functionalized silver nanoislands under myoblast cells is depicted when a 2HZ/5V square wave voltage pulse is on and off. Note that the signal decreases as the voltage is turned on, suggesting that nanoislands are being pulled apart. It should also be noted that the signal of benzenethiolate dominates the spectra and there is a minimum amount of cross talk from the other materials on the substrate (cells/PDMS/PMMA). Vibrational modes for benzenethiol are labeled using Wilson notation for benzene derivatives.<sup>1</sup>

- (1) Wilson, E. B. The Normal Modes and Frequencies of Vibration of the Regular Plane Hexagon Model of the Benzene Molecule. *Phys. Rev.* **1934**.